NANO LETTERS

2009
Vol. 9, No. 10
3406-3412

The Nature of Transport Variations in Molecular Heterojunction Electronics

Jonathan A. Malen,[†,‡,¶] Peter Doak,[‡,§,¶] Kanhayalal Baheti,[‡,§,¶] T. Don Tilley,[§,||] Arun Majumdar,[*,†,‡,⊥,▽] and Rachel A. Segalman[*,‡,⊥,#]

Department of Mechanical Engineering, Department of Chemistry, Applied Science and Technology Program, Department of Chemical Engineering, Department of Materials Science and Engineering, University of California Berkeley, Berkeley, California 94720, and Materials Science Division, Chemical Science Division, Lawrence Berkeley Laboratory, Berkeley, California 94720

Received April 30, 2009; Revised Manuscript Received July 24, 2009

ABSTRACT

Transport fluctuations and variations in a series of metal-molecule-metal junctions were quantified through measurements of their thermopower. Thiol bound aromatic molecules of various lengths and degrees of freedom were chosen to understand the magnitude and origins of the variations. Junction thermopower was determined by measuring the voltage difference across molecules trapped between two gold contacts held at different temperatures. While any given measurement was remarkably stable, the breadth of distributions from repeated measurements implies variations in the offset of the highest occupied molecular orbital (HOMO) relative to the Fermi Energy of the contacts, similar in magnitude to the nominal offset itself. Statistical analysis of data shows that these variations are born at the junction formation, increase with molecular length, and are dominated by variations in contact geometry and orbital hybridization, as well as intermolecular interactions.

Single molecule circuits represent a lower limit on the scalability of electronic devices and are hence an ultimate goal of nanotechnology.[1,2] As circuits approach the nanoscale, transport variations overwhelm ensemble averages and play a more critical role. While important experimental and theoretical advances over the past decade have yielded some insight into electron transport in metal−molecule−metal junctions,[1−13] the nature of variability from junction to junction, fluctuations of a single junction, and stochastic switching remain largely mysterious. We herein quantify the magnitude and origins of these variations through a systematic examination of junction thermopower (S) for prototypical molecular circuits.

Experimental study has hitherto centered on the electronic conductance of single or small numbers of molecules trapped between metal electrodes. Pioneering molecular conductance measurements focused on Au-1,4-benzenedithiol (BDT)-Au junctions.[3,11] Due to π conjugation and the robust Au-thiol bond, this junction showed promise for high conductance applications. However, these experiments yielded vast disagreement in the low-voltage conductance of BDT with values ranging from $6 \times 10^{-4}G_0$ (ref 3) to $1.1 \times 10^{-2}G_0$ (ref 11), where $G_0 = 2e^2/h$ is the fundamental quantum of conductance. Measurements have since shown that the spread in conductance data for BDT is large compared to other molecular junctions.[7,14] Fluctuations in the apparent height of phenylene-ethynylene oligomers and long chain alkyldithiols have also been observed by conventional scanning tunneling microscopy (STM).[15−17] These authors propose that fluctuations are caused by variations in the molecule−substrate hybridization, but the presence of a tunneling gap or a nanocrystal contact make apparent height measurements difficult to relate to molecular transport properties. In parallel to the experimental work, a considerable theoretical effort aimed at understanding charge transport in single molecule junctions has predicted an even broader range of conductances for Au-BDT-Au junctions than is experimentally observed.[18−24] In particular, Basch et. al. found that conductance varied by a factor of 10^3 due to the spectral density overlap between the molecular π orbitals and the Au electrode.[6]

Transport variations observed by both experiment and theory inhibit progress toward single molecule devices, and also lead to many fundamental unanswered questions. They

* To whom correspondence should be addressed. E-mail: (A.M.) majumdar@me.berkeley.edu; (R.A.S.) segalman@berkeley.edu.
† Department of Mechanical Engineering, University of California Berkeley.
‡ Materials Science Division, Lawrence Berkeley Laboratory.
§ Department of Chemistry, University of California Berkeley.
|| Chemical Science Division, Lawrence Berkeley Laboratory.
⊥ Applied Science and Technology Program, University of California Berkeley.
Department of Chemical Engineering, University of California Berkeley.
▽ Department of Materials Science and Engineering, University of California Berkeley.
¶ These authors contributed equally to this work.

10.1021/nl9013875 CCC: $40.75
Published on Web 08/27/2009

are the following: (a) How large are these variations relative to nominal transport properties? (b) How are the observed variations related to variations in the parameters that define transmission, i.e., orbital alignment offset and contact coupling? (c) Are experimentally observed measurement distributions a result of fluctuations within an evolving junction or variations between serially measured junctions? (d) What are the origins of the distributions? Given the preexisting literature and difficulty in measuring the conductance of thiol bound molecules, we have chosen to cite the existing literature values for conductance and not repeat these measurements. Instead we consider junction thermopower, which is a robustly proven experimental probe of electronic transport in molecular junctions.[10,25−27] There has also been renewed interest in the theory of thermopower in molecular junctions. Pauly and co-workers predict that while conductance decays exponentially with increasing molecular length, thermopower should have a linear dependence.[28] This dependence has been shown experimentally, as well.[10,27] Dubi et al. examined the nonequilibrium nature of thermoelectricity and showed that unexpected properties such as sign sensitivity and resonant structure emerge.[29] Ke et al. developed a computationally efficient tool, based on a single particle green function combined with density functional theory, to predict thermopower for a range of thiol bound aromatic molecules.[30] Their prediction of thermopower is also in close agreement with our experimental measurements.[10,26] We now unveil the nature of transport variations by a quantitative comparison of observed thermopower distributions for a series of molecules with varied length and internal degrees of freedom.

Variations in junction conductance and thermopower result from changes in the alignment offset and/or coupling of molecular orbitals with continuum electrode states. In the Landauer formalism charge carriers transmit through the molecular junction with an energy-dependent probability defined by the transmission function $\tau(E)$. Transport is dominated by the highest occupied molecular orbital (HOMO) and lowest unoccupied molecular orbital (LUMO). These states shift and broaden from discrete orbitals due to mixing with the continuum states in the contacts. Peaks in $\tau(E)$ exist where the density of states of the junction is comprised of HOMO or LUMO character. Free carriers in the contacts exist at the chemical potential (E_F in Au), and hence the junction conductance is defined in terms of $\tau(E)$ as follows

$$G \approx \frac{2e^2}{h}\tau(E)\Big|_{E=E_F} = \tau(E)\Big|_{E=E_F} G_0 \qquad (1)$$

where G_0 is the fundamental quantum of conductance.

When a temperature difference ΔT exists between the two contacts, a thermoelectric voltage V is generated. The junction thermopower or Seebeck coefficient (S) relates the voltage produced to the applied temperature bias, $V = S\Delta T$. Butcher extended Landauer formalism to define S in terms of $\tau(E)$ as

$$S = -\frac{\pi^2 k_B^2 T}{3e}\frac{1}{\tau(E)}\frac{\partial \tau(E)}{\partial E}\Big|_{E=E_F} \qquad (2)$$

where e is the charge of a proton, k_B is the Boltzmann constant, and T is the average absolute temperature of the junction.[31]

The energy distribution of $\tau(E)$ in metal−molecule−metal junctions can be described by Lorentzian-shaped peaks at energies related to the HOMO and LUMO energies. Lorentzian peaks are accurate representations of $\tau(E)$ if the density of states in the contacts is constant and weakly coupled to the molecular orbitals.[32] While these conditions are not strictly met in real molecular junctions, the Lorentzian form has been substantiated by more rigorous calculations[25,33] and is a useful tool for analysis.[26,27,34] A general expression for a Lorentzian transmission function is

$$\tau(E) = \sum_{i=1}^{2} \frac{\Gamma_{i,1}\Gamma_{i,2}}{(E - E_i)^2 + (\Gamma_{i,1} + \Gamma_{i,2})^2/4} \qquad (3)$$

where E_i are the energies of the HOMO and LUMO (respectively), and $\Gamma_{i,1}$ and $\Gamma_{i,2}$ are the broadenings of the ith molecular orbitals due to coupling with contacts 1 and 2. These parameters change due to variations in the junction's structure and surroundings that effect transport and can be thereby studied through measurements of thermopower or conductance.

Thermopower measurements were made on BDT, 4,4′-dibenzenedithiol (DBDT), 4,4″-tribenzenedithiol (TBDT) and 2′,5′-dimethyl-4,4″-tribenzenedithiol (DMTBDT) using the modified STM setup described previously[10,26,27] and illustrated in Figure 1 (see Supporting Information for further details on the measurement method and synthetic procedures). One or a few molecules were captured between a Au tip held at ambient temperature and a heated Au substrate held at ΔT above the ambient temperature. The induced thermoelectric voltage V was measured between the tip and the substrate. To create a consistent bandwidth for characterization of transport fluctuations, the acquired voltage was sampled at 10 kHz and passed through a low pass filter set to 1 kHz. Statistics were accumulated through roughly 500 serial approach-withdrawal sequences (AWS) at each ΔT for $\Delta T \sim 0$, 5, 10, 15, 20, and 30 K. For each ΔT, the temperature of the substrate approached steady state and varied by less than 0.2 K during the measurement period. Since we are observing the dependence of V on ΔT, the baseline noise and voltage offset of the amplifier, which are independent of ΔT, do not influence our results. Voltage traces for two consecutive AWSs are shown in red as a function of tip distance in Figure 2; shading indicates the existence of a junction, and V_n and V_{n+1} indicate the mean of each AWS. Control measurements were performed with pure toluene without molecules and representative voltage traces are shown in blue in Figure 2.

Histograms of V taken at each ΔT were built using an automated procedure without any data preselection and then normalized for presentation on a common axis. In the rare case that a molecule was not captured the data was not

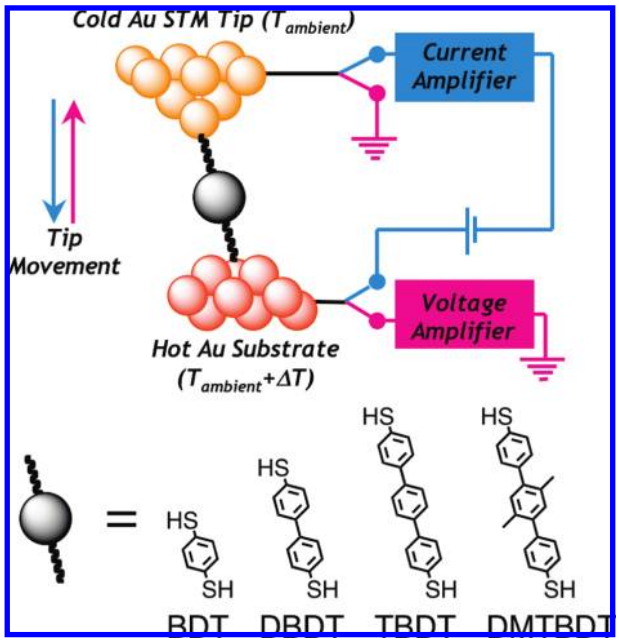

Figure 1. Experimental setup. Schematic of the experimental setup for measuring thermoelectric voltage with a modified STM break junction. Molecules of BDT, DBDT, TBDT, or DMTBDT are captured between the Au STM tip held at ambient temperature and a heated Au substrate held at ΔT above the ambient temperature. As the STM tip approaches a voltage bias is applied between the tip and substrate, and current is monitored to calculate conductance. Once a threshold conductance of $0.01G_0$, indicating formation of a molecular junction, is reached, the tip is withdrawn. During the withdrawal stage, a switch disconnects the voltage bias and current amplifier in favor of a voltage amplifier. The induced thermoelectric voltage V is measured as the tip withdraws before the junction breaks.

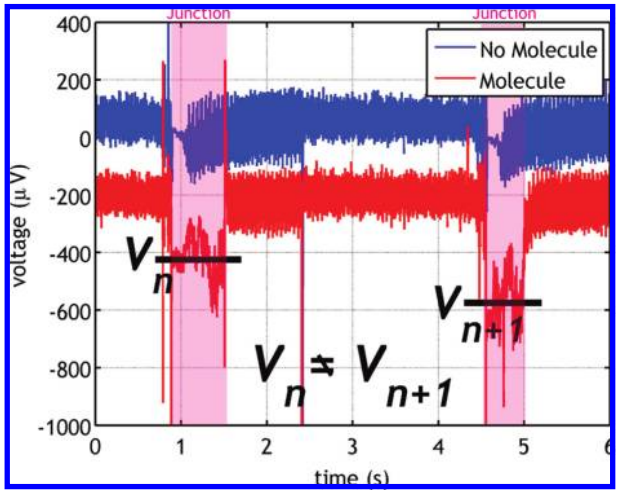

Figure 2. Sample voltage traces. Voltage traces for two consecutive molecular junctions are shown as a function of tip distance in red. For clarity these traces are shifted by -200 μV relative to the blue traces that show control measurements without molecules. V_n and V_{n+1} indicate the differing means of the two consecutive molecular junctions. Observed fluctuations in the thermopower have contributions from fluctuations within an evolving junction, and variations between junctions.

omitted. These are shown in Figure 3a−d, where (a) is BDT, (b) is DBDT, (c) is TBDT, and (d) is DMTBDT. The histograms broaden and shift to the right as higher ΔT are applied. Secondary peaks, found at lower voltage, are clearly discernible for the TBDT and DMTBDT junctions at high ΔT. The peak values of the raw histograms, V_{peak} are plotted as a function of ΔT in Figure 3e−h (circles). The value of V_{peak} increases linearly with ΔT, as has been previously demonstrated.[10,26,27] For TBDT and DMTBDT, only the primary peak values are displayed because the secondary peaks are irresolvable at lower ΔT. Linear fits found by least-squares regression are shown. The slopes of these fits are the junction thermopower S and the 95% confidence interval in slope is the reported error in S, as listed in Table 1. For BDT, DBDT, and TBDT reported values of S are within the error of previously published values.[10,26,27]

The broadening of the voltage histograms with increasing ΔT results from the variation in junction thermopower ΔS, multiplied by an increasing ΔT. In order to study transport variations, the full width at half maxima (FWHM) of the voltage histograms are plotted as a function of ΔT in Figure 3e−h (squares). Secondary peaks of TBDT and DMTBDT were included in the FWHM to capture the total variation in the measured voltage. The FWHM is approximately linear with ΔT and has been fit by linear regression. The slopes of the fits have units of μV/K and are termed ΔS, which can be understood as the observed variation in the thermopower. Instrument noise is small relative to the measured FWHM and does not contribute to ΔS because it is invariant for all ΔT. Histograms of the instrument noise are shown in Figure 1 of the Supporting Information.

Variations in thermopower can be related to orbital offset and contact coupling by considering how perturbations in E_i, $\Gamma_{i,1}$, and $\Gamma_{i,2}$ (ΔE_i, $\Delta\Gamma_{i,1}$, and $\Delta\Gamma_{i,2}$) effect S and G. Variations in thermopower, termed ΔS, are related to these perturbations by first order Taylor expansion

$$\Delta S = \sum_i^2 [\Delta E_i(\partial S/\partial E_i)_{\Gamma_{i,1},\Gamma_{i,2}} + \Delta\Gamma_{i,1}(\partial S/\partial\Gamma_{i,1})_{E_i,\Gamma_{i,2}} + \Delta\Gamma_{i,2}(\partial S/\partial\Gamma_{i,2})_{E_i,\Gamma_{i,1}}] \quad (4)$$

where ΔE_i, $\Delta\Gamma_{i,1}$, and $\Delta\Gamma_{i,2}$ can be positive or negative. In the case of junctions which feature (i) HOMO dominated transmission $(E_F - E_{HOMO})^2 \ll (E_F - E_{LUMO})^2$ and (ii) not too strongly coupled contacts $(E_F - E_{HOMO})^2 \gg (\Gamma_{HOMO,1} + \Gamma_{HOMO,2})^2/4$ (i.e, $\Gamma_{HOMO,1\&2} < 0.5$ eV for the molecules studied), substitution of eqs 2 and 3 into eq 4 yields the following simplified expression

$$\frac{\Delta S}{S} \approx \frac{\Delta E_{HOMO}}{(E_F - E_{HOMO})} \quad (5)$$

This expression relates the normalized variation in thermopower $\Delta S/S$ to the normalized variation in the offset of the HOMO to the Fermi energy of the contacts $\Delta E_{HOMO}/(E_F - E_{HOMO})$. Criteria (i) and (ii) are met by our molecules as discussed in the Supporting Information. Hence, a remarkably large variation in the HOMO transmission peak of benzenedithiols is implied by these measurements of $\Delta S/S$. Values of $\Delta E_{HOMO}/(E_F - E_{HOMO})$ range from 0.3−0.84 dependent

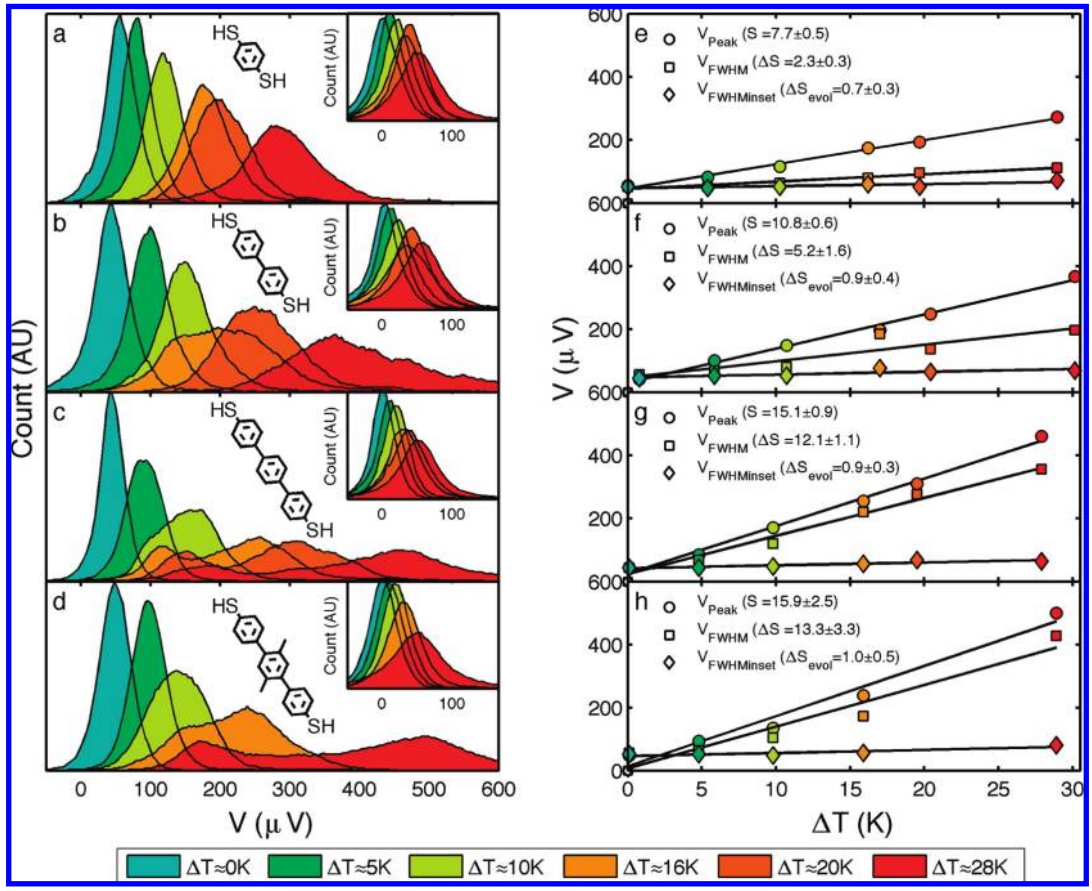

Figure 3. Voltage histograms and linear fits. (a−d) Normalized voltage histograms for ∼500 consecutive junctions at each ΔT for (a) BDT, (b) DBDT, (c) TBDT, and (d) DMTBDT. (insets) Resultant histograms when variations between the mean voltages of each junction are removed, and we are left only with high frequency fluctuations of voltage about each mean. Since the mean of each voltage measurement was subtracted, these histograms should be centered at zero, but have been offset for clarity. (e−h circles) Histogram peaks as a function of ΔT for (a−d). (e−h squares) Histogram full width at half-maximum (FWHM) as a function of ΔT for (a−d). (e−h diamonds) Inset histogram FWHMs as a function of ΔT for (a−d inset). The measured voltage peaks and FWHMs vary linearly with ΔT and slopes are reported as thermopower and fluctuations in thermopower, that is, S, ΔS, and ΔS_{evol}. The reported error in these values is the 95% confidence interval in the slope. ΔS_{evol} represents the fluctuation in S during the evolution of a given junction. Although unshown, $\Delta S_{junc-junc} = \Delta S - \Delta S_{evol}$ represents the variation in S from junction-to-junction differences.

Table 1. Measured Values of S, ΔS, ΔS_{evol}, and $\Delta S_{junc-junc}$ and Relative Variations in the HOMO Calculated by Equation 5 for BDT, DBDT, TBDT, and DMTBDT[a]

	S (μV/K)	ΔS (μV/K)	ΔS_{evol} (μV/K)	$\Delta S_{junc-junc}$ (μV/K)	$(\Delta E)/(E_F - E_{HOMO})$	$(\Delta E_{evol})/(E_F - E_{HOMO})$	$(\Delta E_{junc-junc})/(E_F - E_{HOMO})$
BDT	7.7 ± 0.5	2.3 ± 0.3	0.7 ± 0.3	1.6 ± 0.4	0.30 ± 0.04	0.09 ± 0.04	0.21 ± 0.06
DBDT	10.8 ± 0.6	5.2 ± 1.6	0.9 ± 0.4	4.3 ± 1.6	0.48 ± 0.15	0.08 ± 0.04	0.40 ± 0.16
TBDT	15.1 ± 0.9	12.1 ± 1.1	0.9 ± 0.3	11.2 ± 1.1	0.80 ± 0.09	0.06 ± 0.02	0.74 ± 0.09
DMTBDT	15.9 ± 2.5	13.3 ± 3.3	1.0 ± 0.5	12.3 ± 3.3	0.84 ± 0.25	0.06 ± 0.03	0.77 ± 0.25

[a] The reported error in these values represents the 95% confidence interval.

on the molecular length and are reported in Table 1. Variations in this energy offset are similar in magnitude to the initial offset itself. Energy spans of this size can only result from significant fluctuations in the junction structure and local environment.

Variations in thermopower are large, but still smaller than prior reports of conductance variations, for example, $\Delta S/S \approx 0.3$ for BDT, while the minimum reported variation of conductance for BDT is $\Delta G/G \approx 1.0$.[11] Equation 5 shows that the normalized variation in thermopower $\Delta S/S$ is independent of $\Delta\Gamma$. Under the same criteria used to develop eq 5 a similar relationship for conductance is

$$\frac{\Delta G}{G} \approx \frac{\Delta\Gamma_{HOMO,1}}{\Gamma_{HOMO,1}} + \frac{\Delta\Gamma_{HOMO,2}}{\Gamma_{HOMO,2}} + \frac{2\Delta E_{HOMO}}{(E_F - E_{HOMO})} \quad (6)$$

which implies that variations in conductance are caused by both variations in contact coupling $\Delta\Gamma_{HOMO}$ and offset ΔE_{HOMO} of the HOMO. Thermopower is thus less sensitive to contact coupling than conductance and can be used as a robust probe of ΔE_{HOMO}. More detailed derivations of eqs 5 and 6 are provided in the Supporting Information.

Perhaps the most interesting trend is the increasing magnitude of $\Delta S/S$ with increased molecular length. Conductance histograms of benzenediamines show a similar trend as rings are added; reported $\Delta G/G$ for 1,4′-benzenediamine, 4,4′-dibenzenediamine, and 4,4″-tribenzenediamine are 0.8,

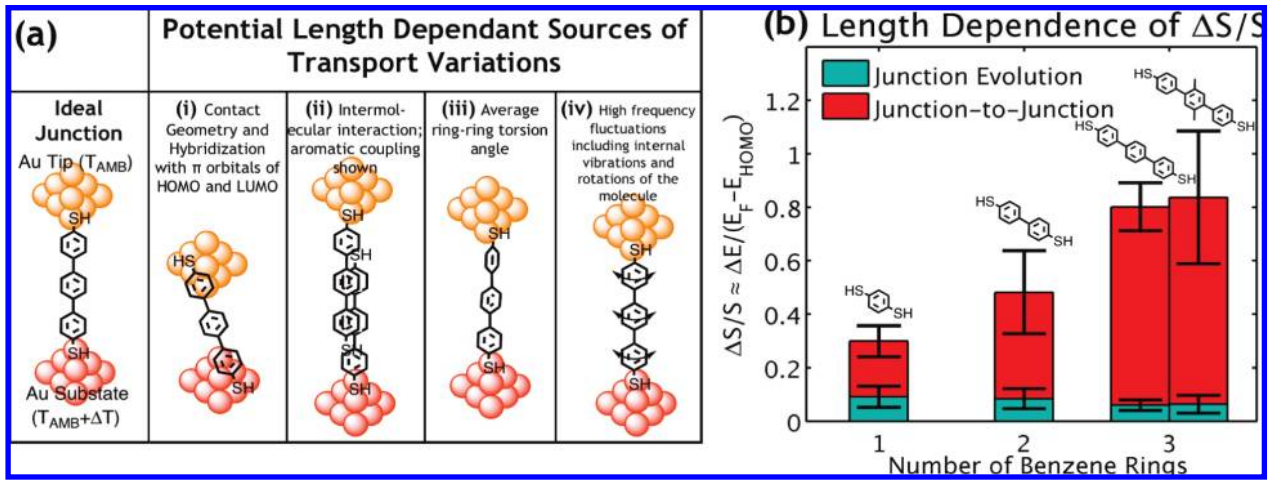

Figure 4. The origins and magnitude of transport fluctuations quantified by $\Delta S/S$. (a) Potential sources of transport fluctuations are illustrated as deviations from an ideal junction. Each of these sources has increased variability with molecular length. (b) $\Delta S/S$ plotted as a function of molecular length and separated into fluctuations during a given junction's evolution and fluctuations from junction-to-junction. Error bars represent the 95% confidence interval of $\Delta S/S$ based on the individual errors in ΔS and S. The increasing magnitude of $\Delta S/S$ with molecular length is consistent with increasing variability in the sources of fluctuations. The lifetime of a junction is ~1 s, but high frequency fluctuations, characteristic of source (iv), are underestimated due to the limited bandwidth of our measurement system (1 kHz). Junction evolutions are a small portion of $\Delta S/S$, indicating that during their lifetime, junctions are stable to low frequency fluctuations from sources (i), (ii), and (iii). Junction-to-junction variations dominate $\Delta S/S$, suggesting that major deviations between junctions are born at the junction formation. Hindered ring−ring rotation in DMTBDT limits the possible ring−ring torsion angles relative to TBDT. Equivalence of $\Delta S/S$ for TBDT and DMTBDT suggests that fluctuations due to average ring−ring torsion angle (iii) are small. Hence, the observed transport fluctuations are born at the junction formation and dominated by sources (i) and (ii).

1.8, and 4.2, respectively.[9] The physical source of the variations is thus dependent on length. Longer molecules can explore more contact geometries resulting in a wider variation of orbital hybridization than shorter molecules. Longer molecules are also more conducive to intermolecular interaction such as aromatic $\pi-\pi$ coupling.[35,36] Furthermore, the number of average ring−ring torsion angles is increased with molecular length, as are the thermally activated vibrational and rotational states of the molecule. Hence, the possible length dependent sources of variation include (i) junction contact geometry and hybridization with molecular orbitals, (ii) intermolecular interactions such as aromatic coupling, (iii) average ring−ring torsion angle in multiring molecules, and (iv) high frequency fluctuations including internal vibrations and rotations of the molecule. These sources are illustrated in Figure 4a as alternatives to the ideal junction generally considered in the literature.

In order to narrow down the origins of the observed fluctuations, we statistically separated ΔS into fluctuations within an evolving junction and variations between serially measured junctions. The voltage traces in Figure 2 show that the mean thermoelectric voltage of consecutive junctions is different ($V_n \neq V_{n+1}$). Deviation between the mean voltages is a result of junction-to-junction variations. Alternatively, deviation of the data about a given mean results from junction-evolutions as the tip is being withdrawn. We emphasize that the voltage amplifier's limited bandwidth (1kHz) results in an averaging of junction-evolutions. To separate these two contributions, the mean voltage for each junction was subtracted from the associated voltage trace, so that all the remaining variation was entirely due to junction evolution. After subtracting the means, the voltage histograms were reconstructed and plotted in the inset of Figure 3a−d. Since the mean of each voltage measurement was subtracted, these histograms should be centered at zero but have been offset for clarity. The FWHM of the inset histograms are plotted as a function of ΔT in Figure 3e−h (diamonds); dependence on ΔT is reduced relative to the original histograms. The slopes of the linear fits represent the fluctuations in thermopower due to junction-evolutions ΔS_{evol}. The fluctuation in S due to junction-to-junction variations $\Delta S_{junc-junc}$ is the difference between ΔS and ΔS_{evol} ($\Delta S_{junc-junc}=\Delta S - \Delta S_{evol}$). Values of ΔS_{evol}, $\Delta S_{junc-junc}$, and the associated normalized fluctuations in E_{HOMO} are listed in Table 1.

Figure 4b shows the total $\Delta S/S$ as a function of molecular length, broken into contributions from ΔS_{evol} and $\Delta S_{junc-junc}$. Comparison of $\Delta S_{evol}/S$ (blue) and $\Delta S_{junc-junc}/S$ (red) reveals that the observed transport fluctuations are largely caused by junction-to-junction variations. These contributions have hitherto been combined and never before quantified for thiols, although qualitative inspection of conductance traces has lead authors to a similar conclusion for BDT alone.[14] Junction evolutions are a small portion of $\Delta S/S$, indicating that during their lifetime, junctions are stable with respect to low frequency fluctuations from sources (i), (ii), and (iii) pictured in Figure 4a. The lifetime of a junction is ~1 s, but high frequency fluctuations, likely prevalent during a junction's evolution, are underestimated due to the limited bandwidth of our measurement system (1kHz). Calculations suggest that picosecond thermal fluctuations of the Au−Au and Au−molecule bonds create a broad distribution of conductance,[37] but unfortunately these fluctuations cannot be resolved by our instruments.

Junction-to-junction variations dominate $\Delta S/S$, suggesting that major deviations between junctions are born at the

junction formation due to sources (i), (ii), or (iii). Equivalence of $\Delta S/S$ for TBDT and DMTBDT suggests that variations due to the ring−ring torsion angle pinning (source (iii)) are small. In contrast, prior work on benzenediamines suggested that conductance variations increase with molecular length due to an increased range of possible ring−ring torsion angles.[9] Relative to TBDT, the ring−ring torsion angles of DMTBDT have a limited range of freedom due to steric hindrance of the methyl groups and are more likely to be pinned in a smaller range of torsion angles.

Contact geometry and orbital hybridization have been credited as the source of transport variations by several theoretical investigations.[6,18−24,33] For example, Basch et al. found that hybridization variations in thiols caused conductance to vary by a factor of 10^3 (ref 6), and Quek et al. found that calculations with 15 distinct Au contact geometries reproduced the observed spread in benzenediamine conductance data.[33] In practice, the spontaneously changing thiol−gold surface morphology,[38−41] as well as the restructuring that results from repeated junction formation and breakage leads to a wide array of junction geometries. Longer molecules can more thoroughly explore the contact morphology to hybridize in a wider range of orientations, while still maintaining an end group exposed for capture by the STM tip. This conclusion is substantiated by recent studies which found that longer alkanes were more likely to create molecular junctions than short alkanes.[42,43]

Intermolecular interactions cannot be ruled out as a source of the observed fluctuations. A recent study of conductance in oligo-phenylene ethynlene molecules established that junctions were still formed when one of the end groups was displaced or fully removed.[36] The authors observed distinct and different conductance peaks in the absence of end groups and concluded that aromatic $\pi-\pi$ coupling between adjacent molecules created controlled molecular bridges between nearby electrodes. Secondary peaks in the voltage histograms of TBDT and DMTBDT, shown in Figure 3c,d, are suggestive of a distinct and different transport channel. The emergent second peak, resolvable only at higher ΔT, suggests a thermopower of $\sim 5.0 \pm 1.0$ μV/K for both TBDT and DMTBDT. A secondary peak was not exhibited by BDT or DBDT. Our results agree with Azzam et al., which showed that strong intermolecular interaction of tribenzene backbones yields well-ordered self-assembled monolayers that do not develop with dibenzene molecules.[35]

By identifying the nature of transport variations in molecular junctions, we open the door to improved molecular electronics design. For thiol bound aromatic junctions, the breadth of observed thermopower distributions implies variations in the offset of the HOMO, relative to E_F of the contacts, similar in magnitude to the nominal offset itself. Statistical analysis of data shows that these variations are born at the junction formation, increase with molecular length, and are dominated by variations in contact geometry and orbital hybridization, as well as intermolecular interactions. To reduce these variations, the development of molecular and organic electronics should focus on fabrication of contact geometry and placement of molecular circuit components onto these contacts such that possibilities available to the molecule are limited. One recent paper suggests the use of fullerene end groups to improve junction stability.[44] Similar innovations directed toward improvement of junction consistency, despite the local contact environment, could take single molecule electronics from interesting model systems to the ultimate frontier of integrated electronics.

Acknowledgment. We gratefully acknowledge support from the Division of Materials Sciences and Engineering in the Department of Energy Basic Energy Sciences (DOEBES) through the Thermoelectrics Program at Lawrence Berkeley National Laboratory (LBNL). We also gratefully acknowledge support in the form of instrumentation from the NSF-NSEC−COINS at UC Berkeley. We thank J. B. Neaton and Su Ying Quek from LBNL for insightful conversations that benefited this work.

Supporting Information Available: Detailed descriptions of the measurement method, synthetic procedures, derivations of eqs 5 and 6, and characterization of instrument noise are included. This material is available free of charge via the Internet at http://pubs.acs.org.

References

(1) Tao, N. J. *Nat. Nanotechnol.* **2006**, *1* (3), 173–181.
(2) Joachim, C.; Ratner, M. A. *Proc. Natl. Acad. Sci. U.S.A.* **2005**, *102* (25), 8801–8808.
(3) Reed, M. A.; Zhou, C.; Muller, C. J.; Burgin, T. P.; Tour, J. M. *Science* **1997**, *278* (5336), 252–254.
(4) Park, H.; Park, J.; Lim, A. K. L.; Anderson, E. H.; Alivisatos, A. P.; McEuen, P. L. *Nature* **2000**, *407* (6800), 57–60.
(5) Xu, B. Q.; Tao, N. J. J. *Science* **2003**, *301* (5637), 1221–1223.
(6) Basch, H.; Cohen, R.; Ratner, M. A. *Nano Lett.* **2005**, *5* (9), 1668–1675.
(7) Venkataraman, L.; Klare, J. E.; Tam, I. W.; Nuckolls, C.; Hybertsen, M. S.; Steigerwald, M. L. *Nano Lett.* **2006**, *6* (3), 458–462.
(8) Venkataraman, L.; Park, Y. S.; Whalley, A. C.; Nuckolls, C.; Hybertsen, M. S.; Steigerwald, M. L. *Nano Lett.* **2007**, *7* (2), 502–506.
(9) Venkataraman, L.; Klare, J. E.; Nuckolls, C.; Hybertsen, M. S.; Steigerwald, M. L. *Nature* **2006**, *442* (7105), 904–907.
(10) Reddy, P.; Jang, S. Y.; Segalman, R. A.; Majumdar, A. *Science* **2007**, *315* (5818), 1568–1571.
(11) Xiao, X. Y.; Xu, B. Q.; Tao, N. J. *Nano Lett.* **2004**, *4* (2), 267–271.
(12) Galperin, M.; Ratner, M. A.; Nitzan, A.; Troisi, A. *Science* **2008**, *319* (5866), 1056–1060.
(13) Nitzan, A.; Ratner, M. A. *Science* **2003**, *300* (5624), 1384–1389.
(14) Ulrich, J.; Esrail, D.; Pontius, W.; Venkataraman, L.; Millar, D.; Doerrer, L. H. *J. Phys. Chem. B* **2006**, *110* (6), 2462–2466.
(15) Donhauser, Z. J.; Mantooth, B. A.; Kelly, K. F.; Bumm, L. A.; Monnell, J. D.; Stapleton, J. J.; Price, D. W.; Rawlett, A. M.; Allara, D. L.; Tour, J. M.; Weiss, P. S. *Science* **2001**, *292* (5525), 2303–2307.
(16) Ramachandran, G. K.; Hopson, T. J.; Rawlett, A. M.; Nagahara, L. A.; Primak, A.; Lindsay, S. M. *Science* **2003**, *300* (5624), 1413–1416.
(17) Moore, A. M.; Dameron, A. A.; Mantooth, B. A.; Smith, R. K.; Fuchs, D. J.; Ciszek, J. W.; Maya, F.; Yao, Y. X.; Tour, J. M.; Weiss, P. S. *J. Am. Chem. Soc.* **2006**, *128* (6), 1959–1967.
(18) Bratkovsky, A. M.; Kornilovitch, P. E. *Phys. Rev. B* **2003**, *67* (11), 115307.
(19) Di Ventra, M.; Pantelides, S. T.; Lang, N. D. *Phys. Rev. Lett.* **2000**, *84* (5), 979–982.
(20) Emberly, E. G.; Kirczenow, G. *Phys. Rev. B* **1998**, *58* (16), 10911–10920.
(21) Hall, L. E.; Reimers, J. R.; Hush, N. S.; Silverbrook, K. *J. Chem. Phys.* **2000**, *112* (3), 1510–1521.
(22) Stokbro, K.; Taylor, J.; Brandbyge, M.; Mozos, J. L.; Ordejon, P. *Comput. Mater. Sci.* **2003**, *27* (1−2), 151–160.

(23) Ke, S. H.; Baranger, H. U.; Yang, W. T. *J. Chem. Phys.* **2005**, *122* (7), 074704.
(24) Ke, S. H.; Baranger, H. U.; Yang, W. T. *J. Chem. Phys.* **2005**, *123* (11), 114701.
(25) Paulsson, M.; Datta, S. *Phys. Rev. B* **2003**, *67* (24), 241403.
(26) Baheti, K.; Malen, J. A.; Doak, P.; Reddy, P.; Jang, S. Y.; Tilley, T. D.; Majumdar, A.; Segalman, R. A. *Nano Lett.* **2008**, *8* (2), 715–719.
(27) Malen, J. A.; Doak, P.; Baheti, K.; Tilley, T. D.; Segalman, R. A.; Majumdar, A. *Nano Lett.* **2009**, *9* (3), 1164–1169.
(28) Pauly, F.; Viljas, J. K.; Cuevas, J. C. *Phys. Rev. B* **2008**, *78* (3), 035315.
(29) Dubi, Y.; Di Ventra, M. *Nano Lett.* **2009**, *9* (1), 97–101.
(30) Ke, S. H.; Yang, M.; Curtarolo, S.; Baranger, H. U. *Nano Lett.* **2009**, *9* (3), 1011–1014.
(31) Butcher, P. N. *J. Phys.: Condens. Matter* **1990**, *2* (22), 4869–4878.
(32) Datta, S. *Quantum transport: atom to transistor*; Cambridge University Press: Cambridge, 2005; pp xiv, 404.
(33) Quek, S. Y.; Venkataraman, L.; Choi, H. J.; Loule, S. G.; Hybertsen, M. S.; Neaton, J. B. *Nano Lett.* **2007**, *7* (11), 3477–3482.
(34) Kittel, C.; McEuen, P. *Introduction to solid state physics*, 8th ed.; J. Wiley: Hoboken, NJ, 2005; pp xix, 680.
(35) Azzam, W.; Wehner, B. I.; Fischer, R. A.; Terfort, A.; Woll, C. *Langmuir* **2002**, *18* (21), 7766–7769.
(36) Wu, S. M.; Gonzalez, M. T.; Huber, R.; Grunder, S.; Mayor, M.; Schonenberger, C.; Calame, M. *Nat. Nanotechnol.* **2008**, *3* (9), 569–574.
(37) Andrews, D. Q.; Van Duyne, R. P.; Ratner, M. A. *Nano Lett.* **2008**, *8* (4), 1120–1126.
(38) Cometto, F. P.; Paredes-Olivera, P.; Macagno, V. A.; Patrito, E. M. *J. Phys. Chem. B* **2005**, *109* (46), 21737–21748.
(39) Esplandiu, M. J.; Carot, M. L.; Cometto, F. P.; Macagno, V. A.; Patrito, E. M. *Surf. Sci.* **2006**, *600* (1), 155–172.
(40) Mccarley, R. L.; Dunaway, D. J.; Willicut, R. J. *Langmuir* **1993**, *9* (11), 2775–2777.
(41) Stranick, S. J.; Parikh, A. N.; Allara, D. L.; Weiss, P. S. *J. Phys. Chem.* **1994**, *98* (43), 11136–11142.
(42) Jang, S. Y.; Reddy, P.; Majumdar, A.; Segalman, R. A. *Nano Lett.* **2006**, *6* (10), 2362–2367.
(43) Kamenetska, M.; Koentopp, M.; Whalley, A. C.; Park, Y. S.; Steigerwald, M. L.; Nuckolls, C.; Hybertsen, M. S.; Venkataraman, L. *Phys. Rev. Lett.* **2009**, *102*, 126803.
(44) Martin, C. A.; Ding, D.; Sorensen, J. K.; Bjornholm, T.; van Ruitenbeek, J. M.; van der Zantt, H. S. J. *J. Am. Chem. Soc.* **2008**, *130* (40), 13198–13199.

NL9013875